DOI 10.1007/s10946-024-10187-5
Journal of Russian Laser Research, Volume 45, Number 1, January, 2024

GENERATION OF DUAL-WAVELENGTH OPTICAL DOMAIN–WALL DARK–BRIGHT PULSES BY COMPOSITE FILTERING EFFECTS

Qingyu Chang

Guangdong-Hong Kong-Macau Joint Laboratory for Intelligent Micro-Nano Optoelectronic Technology Foshan 528000, China

School of Computer Science and Engineering Macau University of Science and Technology Macau 999078, China

E-mail: changqingyu1024@qq.com

Abstract

Optical domain–wall (DW) solitons have attracted considerable attention for their special applications in wavelength-division multiplexing and signal processing in optical communications. In this study, we construct a dispersion-managed fiber laser with a composite filtering effect composed of nonlinear polarization rotation (NPR) filtering and Lyot filtering for achieving dual-wavelength domain–wall dark–bright pulses. Our optical-domain dark–bright pulse is characterized by even, though it has two optical wavelength components, still has the same repetition frequency. The phenomenon of dual-wavelength dark and bright pulses occurs by adjusting the composite filtering, and the dark and bright pulses can be separated by continuing the filtering. Our work presents a novel approach to achieve dual-wavelength domain–wall dark–bright pulses.

Keywords: nonlinear polarization rotation, Lyot filtering, optical domain–wall, dual-wavelength, dark–bright pulses.

1. Introduction

Passive mode-locked fiber lasers (MLFLs) have gained attention due to their all-fiber structure and miniaturization capability. They enable the generation of various pulses, such as h-type pulses [1, 2], dual-wavelength mode-locked pulses [3–5], and soliton molecules, through filter modulation techniques [6]. MLFLs find applications in fiber optic communication, LIDAR, biomedical research, and industrial laser processing [7–9]. The strong filtering effect within the laser cavity provides a platform for studying pulses as nonlinear dynamical phenomena. Among them, there are not many studies on the two special and interesting phenomena of continuous wave (CW) and nonlinear Schrödinger mode solitons (NLSMs) generated through the filtering effect. In addition to the well-known nonlinear Schrödinger equation (NLSE) used to predict soliton properties [10], the gain competition plays a parallel and independent role in determining the soliton dynamics within the optical soliton system of resonant cavities. The gain competition coexists with the NLSE without interference and results in the generation of bright or dark solitons, as well as vectorial bright and dark solitons, regardless of positive or negative dispersion conditions. These unique solitons, known as optical domain–wall pulse solitons, were first proposed theoretically by Haelterman and Sheppard in 1994 [11] and later observed experimentally by Zhang et

Manuscript submitted by the author in English on October 23, 2023.

al. [12]. Optical domain–walls, which have been theoretically predicted [13–15], are local structures that separate the polarization states in birefringent lasers or wavelengths in dual-wavelength lasers. They find important applications in supercontinuum spectroscopy [16], optical communication, and switching [13].

Dual-wavelength optical domain–walls were first proposed by Heitmann et al., where a local structure is formed through interaction between the polarization components or cross-coupling between two wavelengths. Using the polarization methods, it is possible to separate differently polarized eigenstates in a dispersive Kerr medium, resulting in a stable localized structure, known as a polarized domain–wall soliton [17].

Since then, other research teams have further investigated the interaction between two wavelengths with the same polarization eigenstates, leading to the formation of optical domain–walls and solitons with multiple peak distributions [18]. Tang [19] demonstrated the first experimental evidence of dual-wavelength continuous-wave (CW) lasers. Building upon this work, more discoveries have been made in the study of dual-wavelength co-polarized states. In 2012, Ai-Ping Luo et al. observed dual-wavelength domain–wall pulses in an Erbium-doped fiber laser by incorporating a highly nonlinear fiber with a length of approximately 85 m in the cavity. The high nonlinearity enhanced the cross-coupling between the two wavelength components [20]. In the same year, Luo's team, led by Yining Qiu, generated two bands of domain–wall bright and dark pulses in a negative dispersion octave cavity, using a nonlinear amplifying loop mirror (NALM) mode-locked setup [21]. Two years later, Luo's team extended the highly nonlinear fiber (HNLF) by 215 m, increasing the cavity length by 2.37 km, resulting in high-energy dual-wavelength domain–wall pulses with low repetition frequencies [22].

Notably, some research teams have also utilized material mode-locking techniques to observe this phenomenon. For instance, Liu used Carbon nanotubes (CNTs) and Erbium-doped fiber ring lasers to generate dual-wavelength domain–wall dark pulses [23], while Harith Ahmad of the University of Malaya observed dual-wavelength domain–wall dark pulses in a MoS_2-based Ytterbium-doped fiber laser [24]. In 2018 and 2020, Koo J. et al., Korean scholars obtained dual-wavelength dark solitons in a fiber laser, using Bismuth Telluride topological insulators, with pulse widths and repetition frequencies of 10.3 ns and 20.7 MHz, respectively [25]. In 2020, Ahmad Nadi of Beni-Souf University, Egypt argued that these dual-wavelength pulses are not related to different polarizations but rather to two wavelengths associated with "color domains" (CDW) caused by the optical Kerr effect in highly nonlinear fibers. They referred to this phenomenon as cross-gain saturation and cross-polarization coupling [26]. Dual-wavelength optical domain–wall pulses exhibit rich dynamical phenomena and have significant potential for applications in fiber sensing, fiber device testing, ultrafast optics, and optical communications.

In this paper, we focus on investigating the properties of a ring cavity Erbium-doped fiber laser under a composite filtering effect created by utilizing the nonlinear polarization rotation (NPR) technique and Lyot filtering. The objective is to manipulate the generation of dual-wavelength pulses by carefully managing the dispersion of the laser and coupling the composite filtering effect. Our approach involves switching between a dual-wavelength domain–wall dark–bright pulses simply by modulating the pump and polarization controller (PC). Moreover, the dark and bright pulses can be separated by filtering. This novel method allows for the generation of an optical domain–wall pulses under the composite filter effect. By studying the characteristics and dynamics of these dual-wavelength domain–wall pulses, we aim to gain insights into their behavior and explore their potential applications in various fields. Overall, our work presents a new approach for generating optical domain–wall pulses, using the composite filter effect, and show the case of a controllable generation of dual-wavelength pulses through the manipulation of dispersion and filtering techniques.

2. Experimental Setups

In Fig. 1, we show the experimental setup of the fiber laser. The entire cavity length is almost 28.5 m. A 980 nm laser with a maximum power of 400 mW is used to generate signal light in the 1550 nm band by pumping a 2 m long commercial Erbium-doped fiber (EDF) with a gain factor of 20.1 dB/m, through a 980/1550 nm wavelength division multiplexer (WDM). The nonlinear polarization rotation (NPR) effect is generated in the main ring cavity through the synergy of a polarization controller (PC) and a polarization-dependent isolator (PD-ISO). An optimum balance between the dispersion, nonlinearity, loss, gain, filtering, and saturation of absorption is used to generate mode-locked pulses. Also we add a 0.1 m polarization-maintaining fiber (PMF) and two additional PCs to the ring gain cavity to form a Lyot filter, where the PD-ISO acts as a bias initiator and detector. A composite filter effect is formed with the NPR to control the tunable output of the mode-locked pulses. A dispersion compensating fiber (DCF) is added to achieve dispersion management so that the entire cavity is in a near-zero positive dispersion region of 0.668 ps^2.

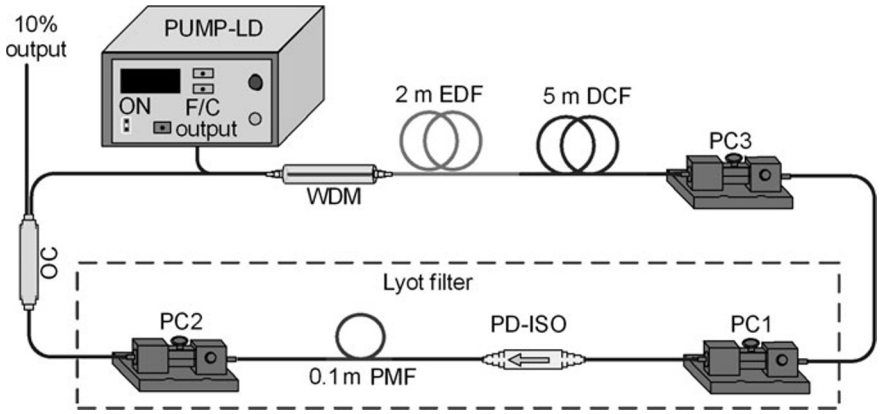

Fig. 1. Experimental setup.

A 1×2 optic coupler with 10% termination is used as the output of the entire fiber laser. We use a spectrum analyzer (OSA, Yokogawa AQ6375B), a 12.5 GHz photodetector (Newport 818-BB-51F), and a 13 GHz oscilloscope (Wavemaster 813Zi-B), as well as a 3 GHz radio spectrum analyzer (Rigol DSA1030). A Spectrum Analyzer with a Newport 818-BB-51F Photodetector, with a bandwidth of 12.5 GHz is used to evaluate the time response, spectra, RF profiles, and autocorrelation traces of the laser pulses (Wavemaster 813Zi-B). Before being fed into the RF preamplifier, an amplifier (frequency-specific LTRAN LOA3000) must be used to amplify the signal to achieve sufficient intensity for autocorrelation measurements based on the second harmonic generation.

We carefully adjust the common composite filters PC1 and PC2 to achieve multi-wavelength cross-coupling and other nonlinear effects to form optical domain–wall dark and bright pulse outputs.

At this point, the NPR filtering transmission function in the cavity can be expressed as follows [27]:

$$T_{\mathrm{NPR}} = \cos^2\theta_1 \cos^2\theta_2 + \sin^2\theta_1 \sin^2\theta_2 + \frac{1}{2}\sin^2 2\theta_1 \sin^2 2\theta_2 \cos^2(\Delta\phi_L + \Delta\phi_{\mathrm{NL}}), \tag{1}$$

$$\Delta\phi_L = 2\pi L(n_y - n_x)/\lambda, \tag{2}$$

$$\Delta\phi_{\mathrm{NL}} = 2\pi n_2 PL\cos(2\theta_1)/(\lambda A_{\mathrm{eff}}), \tag{3}$$

where θ_1 and θ_2 denote the arc formed by the fast axis of the fiber, the deflector, and the detector, respectively, and $\Delta\phi_L$ and $\Delta\phi_{\mathrm{NL}}$ represent the linear and nonlinear phase shifts, respectively. Here, n_x is the refractive index of the fast axis of the fiber, while n_y is the refractive index of the slow axis, L represents the total length of the laser cavity, λ denotes the operating wavelength, n_2 is the nonlinear coefficient, P indicates the input signal's instantaneous power, and A_{eff} is the mode field area. From Eq. (3) follows that

the operational wavelength and the input signal's immediate power cause the transmittance to fluctuate.

In the experiment, both the length and the instantaneous peak power of the single-mode fiber are fixed. The transmittance can be varied with the phase, amplitude, and period. Intracavity birefringence produces an internal spectrum filter that allows for tuning and switching of wavelength laser location and wavelength spacing.

The Lyot-based filtering can be expressed as follows [28]:

$$T_{\mathrm{Lyot}} = \frac{1}{2}\cos^2\left(\frac{\pi\Delta n}{\lambda}L_{\mathrm{PMF}}\right)(1+\sin 2\theta), \tag{4}$$

where Δn, L_{PMF}, and θ represent the birefringence coefficient, the length of the polarization preserving fiber, and the angle between the polarization direction of the incident light and the fast axis of the PMF, respectively.

When the Lyot filters are embedded in the main NPR cavity, they operate simultaneously with a common coupling parameter, the angle between the polarization-dependent isolators, and the fast axis of the SMF, creating a coupled composite filter effect. The composite filtering effect can be expressed as follows:

$$T_{\mathrm{composite}} = T_{\mathrm{NPR}} \cdot T_{\mathrm{Lyot}}. \tag{5}$$

3. Experimental Results and Analysis

By increasing the pump power to 166 mW and accordingly turning the polarization controller (PC), we observe a typical output of dark–bright pulses with two wavelengths. In the frequency domain, the laser operates in the two-wavelength range; see Fig. 2. One wavelength is centered at 1556.6 nm and the other, at 1558.4 nm. The wavelength spacing of the 3 dB spectral bandwidth is approximately equal to 1.82 nm. In addition, the spectrum shows no obvious Kelly sidebands, which can be due to birefringent filtering effects within the cavity. Tang et al. also observed a double wavelength output in a laser and proved that this phenomenon was caused by a filtering effect within the laser [29]. The double wavelength is produced by a combination of laser amplification and a filter effect resulting from birefringence. These two bands compete for the amplification of the laser and, thus, produce two different wavelengths. In our experiment, as the pump power is gradually increased, a notch appears on the oscilloscope amidst the continuous optical background noise of the bright pulses. This notch represents the occurrence of dark–bright pulses at the optical domain–wall, with a pulse spacing of 137 ns. To investigate the emergence of dark–bright pulses generated by a fiber laser with near-zero normal dispersion at the optical domain–wall, we used a Newport TBF-1550-1.0 filter to separately analyze each wavelength; see Fig. 3. Each filtered wavelength corresponds to bright and dark pulses, respectively, with the ratio of bright to dark pulses being 7 : 3. These pulses have the same repetition frequency and remain constant throughout the analysis. The NPR effect is one of the main mechanisms for the generation of dark pulses, which typically occurs in a laser resonator with a polarized environment. The PD-ISO used in our laser resonator exhibits excellent polarization effects and, thus, provides the necessary conditions for generation of dark pulses. Finally, under the influence of nonlinear effects, the dark and bright pulses of the two wavelengths combine through cross-coupling to form the output of optical domain–wall dark–bright pulses.

Moreover, under the same conditions; see Fig. 4, we can observe stable autocorrelation pulses in the middle of a strong continuous-wave background. The pulse train covers the entire scan range of the

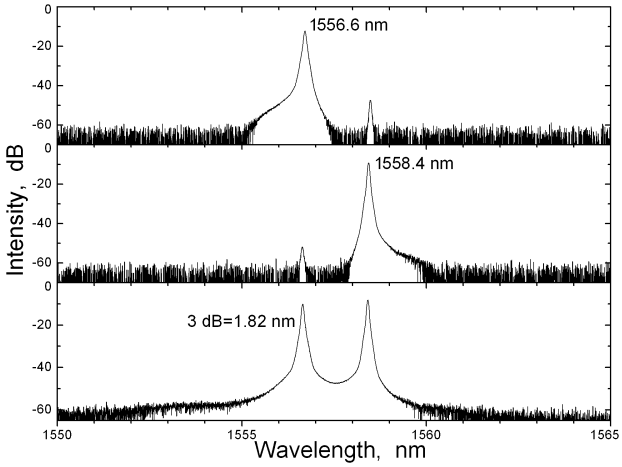

Fig. 2. Dual-wavelength along with filtered spectra.

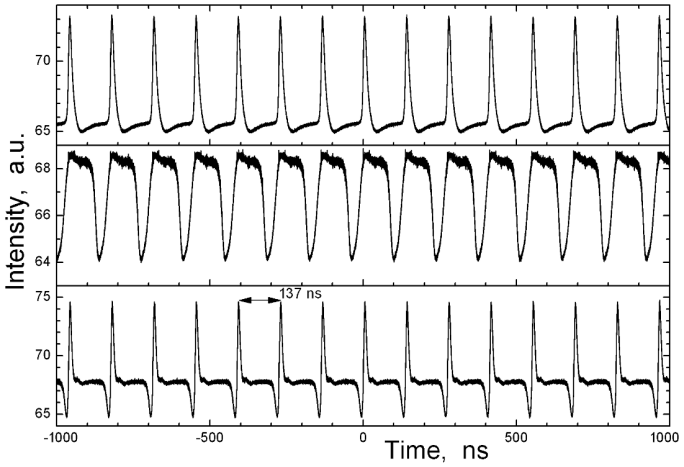

Fig. 3. Dual-wavelength along with filtered pulses.

autocorrelation trace and exhibits some periodic modulation, indicating the presence of dark pulses [30, 31]. Moreover, the experimentally measured spectra according to Fig. 2 show a symmetric profile with uniform wavelength, which is a characteristic feature of fiber lasers with dark solitons [32–34], where the occurrence of multiple peaks in the autocorrelation is due to the high repetition frequency of the pulses. The dark and bright pulses with high repetition frequency are generated by the spontaneous modulation instability (MI) that occurs in the cavity with a near-zero dispersion and a low threshold [35]. In addition, an intensity modulation with a high repetition frequency is introduced into the optical field. In autocorrelation analysis, the dark and bright pulses with a high repetition frequency alternate or overlap, resulting in a periodic structure with different amplitudes or intensities. However, our autocorrelation phenomenon exhibits a certain asymmetry. This is due to the sensitivity of the polarization state of the optical fiber, which can be significantly affected by environmental factors during the experimental autocorrelation measurements. The autocorrelation trace can be made symmetric by adjusting the polarization state. This is the first case where a high repetition rate autocorrelated phenomenon is observed in a pair of bright and dark pulses with two wavelengths, which experimentally supports Tang's theory [36].

As shown in Fig. 5, we record a single spectrum image with a width of 10 MHz and a signal-to-noise ratio of 60 dB. The inset image shows an RF image with a pulse width of 100 MHz and a resolution of

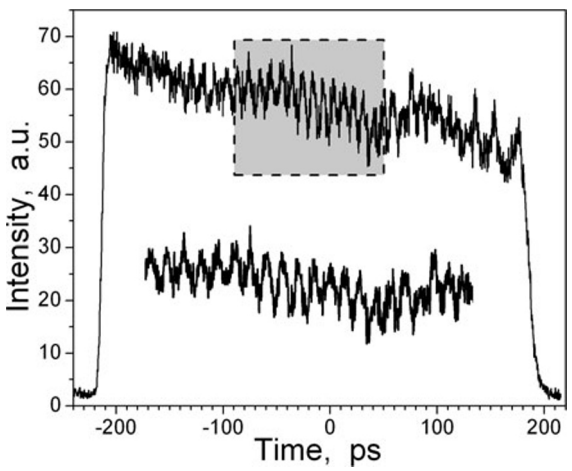

Fig. 4. Autocorrelation.

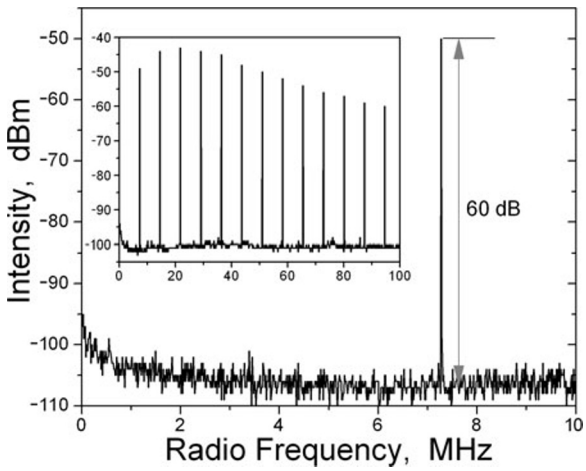

Fig. 5. Radio frequency.

3 kHz. The fundamental frequency observed in the RF image is about 7.3 MHz, which is consistent with the time domain interval. This RF image confirms the stability of the dark–bright pulses obtained in our experiments. Our experimental results indicate that the generation of pulse pairs results from the interaction of bright–dark pulses by intense cross-coupling in two different frequency bands. Even in the case of the two-wavelength spectrum, we observe only one frequency component that is characteristic of typical two-wavelength operation and results from the cross-coupling effect with these two wavelengths. To further investigate this phenomenon, we remove the polarization-maintaining fiber (PMF) and find that the behavior of the dual-wavelength double domain–wall no longer occurs. This indicates that the composite filtering effect plays an important role in the observed behavior.

Moreover, by fixing the intracavity power at 173 nW and regulating PC2, tunable dark–bright pulse pairs with wavelengths ranging from 1561.62 to 1557.79 nm can be obtained, and the spectral separation varies from 2.17 to 2.8 nm with an average of 2.5 nm; see Fig. 6. This indicates that the dark–bright pulses of the optical domain–wall are tunable with two wavelengths.

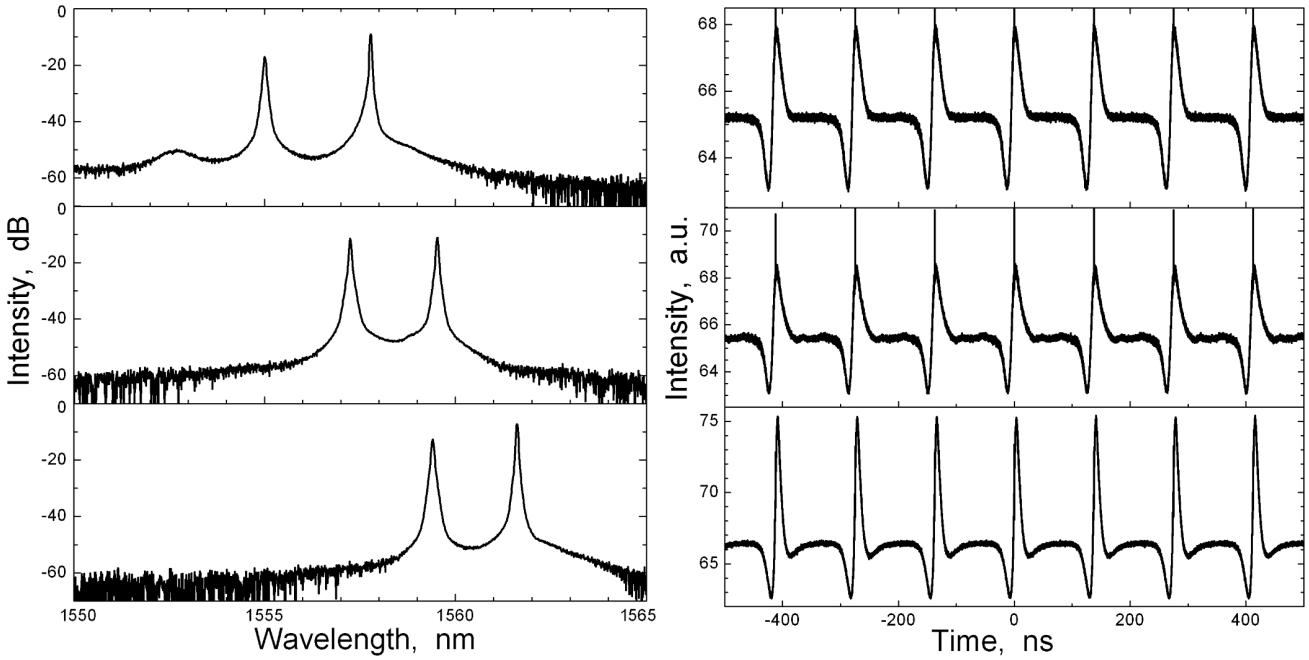

Fig. 6. Tunable dual-wavelength optical domain–wall dark and bright pulse pairs.

4. Conclusions

In summary, our study demonstrates the existence of a dual-wavelength optical domain–wall in fiber lasers under the composite filtering effect with near-zero positive dispersion. The composite filtering effect plays a crucial role in their formation. These optical domain–walls generate a stable sequence of dark–bright pulses in the laser cavity, with a repetition period corresponding to the fundamental frequency of the laser. The formation of these optical domain–wall dark–bright pulses in the optical two-wavelength range is not only influenced by dispersion and nonlinearity, but also significantly affected by cross-phase modulation. Furthermore, we observed a weak modulation on the autocorrelator, where

typical dark–bright pulses are generated within one repetition period of the laser. Our research presents a promising method for generating optical domain–wall pulses that offers significant potential for future applications in optical communication.

References

1. L. Gu, Z. Liu, Y. Shu, et al., *Opt. Laser Technol.*, **157**, 108659 (2023).
2. Z. He, Y. Chen, Z. Deng, et al., *Appl. Phys. Express*, **13**, 012011 (2019).
3. J. Lin, Z. Dong, T. Dong, et al., *Opt. Laser Technol.*, **141**, 107093 (2021).
4. H. R. Yang, *J. Modern Opt.*, **62**, 1363 (2015).
5. C. Zeng, Y. D. Cui, and J. Guo, *Opt. Commun.*, **347**, 44 (2015).
6. B. Liu, Y. Liu, Y. Luo, et al., *Opt. Commun.*, **457**, 124700 (2020).
7. C. Xu and F. W. Wise, *Nat. Photonics*, **7**, 875 (2013).
8. Y. Zhao, P. Guo, X. Li, et al., *Carbon*, **149**, 336 (2019).
9. Q. Zhang, J. Chang, Q. Wang, et al., *Sensors*, **18**, 42 (2018).
10. V. N. Serkin, V. A. Vysloukh, and J. R. Taylor, *Electron. Lett.*, **29**, 12 (1993).
11. M. Haelterman and A. P. Sheppard, *Opt. Lett.*, **19**, 96 (1994).
12. H. Zhang, D. Y. Tang, L. M. Zhao, and R. J. Knize, *Opt. Express*, **18**, 4428 (2010).
13. M. Haelterman and A. P. Sheppard, *Opt. Lett.*, **19**, 96 (1994).
14. M. Haelterman and M. Badolo, *Opt. Lett.*, **20**, 2285 (1995).
15. B. A. Malomed, *Phys. Rev. E*, **50**, 1565 (1994).
16. C. Milián, D. V. Skryabin, and A. Ferrando, *Opt. Lett.*, **34**, 2096 (2009).
17. M. Haelterman and A. P. Sheppard, *Phys. Rev. E*, **49**, 4512 (1994).
18. M. Haelterman and M. Badolo, *Opt. Lett.*, **20**, 2285 (1995).
19. H. Zhang, D. Tang, L. Zhao, and X. Wu, *Opt. Express*, **19**, 3525 (2011).
20. H. Zhang, D. Tang, M. Tlidi, et al., Dispersion-Managed Dark Solitons in Erbium-Doped Fiber Lasers, arXiv:1007.3129 (2010).
21. H. Yin, W. Xu, A. P. Luo, et al., *Opt. Commun.*, **283**, 4338 (2010).
22. H. Y. Wang, W. C. Xu, Z. C. Luo, et al., *Chin. Phys. Lett.*, **28**, 024207 (2011).
23. H. Y. Wang, W. C. Xu, W. J. Cao, et al., *Laser Phys.*, **22**, 282 (2012).
24. H. Ahmad, Z. C. Tiu, A. Zarei, et al., *Appl. Phys. B*, **122**, 15 (2016).
25. H. P. Li, H. D. Xia, Z. Jing, et al., *Laser Phys.*, **22**, 261 (2012).
26. B. Guo, Y. Yao, J. J. Tian, et al., *IEEE Photonics Technol. Lett.*, **27**, 701 (2015).
27. H. A. Haus, *Phys. Today*, **55**, 58 (2002).
28. Z. Zhang, L. Zhan, K. Xu, et al., *Opt. Lett.*, **33**, 324 (2008).
29. H. Zhang, D. Tang, L. Zhao, and X. Wu, *Opt. Express*, **19**, 3525 (2011).
30. A. Nady, G. Semaan, M. Kemel, et al., *J. Lightw. Technol.*, **38**, 6905 (2020).
31. R. Leners, P. Emplit, D. Foursa, et al., *J. Opt. Soc. Am. B*, **14**, 2339 (1997).
32. Y. Meng, S. Zhang, H. Li, et al., *Opt. Eng.*, **51**, 064302 (2012); DOI: 10.1117/1.OE.51.6.064302
33. X. Li, S. Zhang, Y. Meng, and Y. Hao, *Opt. Express*, **21**, 8409 (2013).
34. R. Z. R. R. Rosdin, N. M. Ali, S. W. Harun, and H. Arof, *Int. J. Phys. Math. Sci.*, **8**, 1461 (2014).
35. C. J. S. D. Matos, D. A. Chestnut, and J. R. Taylor, *Opt. Lett.*, **27**, 915 (2002).
36. Y. Tang, *Opt. Lett.*, **39**, 3484 (2014).